# Exergy Analyses of Heat Supply Systems for a Building Cluster with CARNOT

P.M. Falk[1,2,*], F. Dammel[1,2,], P. Stephan[1,2,]

[1]Institute for Technical Thermodynamics, Technische Universität Darmstadt,
Alarich-Weiss-Straße 10, 64287 Darmstadt, Germany
[2]Darmstadt Graduate School of Excellence Energy Science and Engineering,
Jovanka-Bontschits-Straße 2, 64287 Darmstadt, Germany
E-mail: *falk@ttd.tu-darmstadt.de

## Abstract

In this paper, a model to simulate community heating systems is presented and energy and exergy analyses are conducted for a district heating system with three different heat generation alternatives. The alternatives are a gas boiler system, a system assisted by solar thermal collectors with a seasonal thermal energy storage and a gas boiler as backup, and a system with geothermal borehole heat exchangers combined with a heat pump. The heat supply of a building cluster of 11 buildings is dynamically modeled using the MATLAB/Simulink based toolbox CARNOT. The aim is to match the low exergy heating demand with a low exergy heat source. To cover an energy demand of 263.7 MWh/a, the geothermal system needs 174.0 MWh/a of exergy, the solar thermal system 269.2 MWh/a of exergy and the gas boiler system 324.9 MWh/a. A parameter study of the solar thermal system shows better results for lower supply temperatures and a lower heat loss coefficient $k$, but the results depend strongly on the chosen storage size. It was found that the use of fossil fuel could be reduced by 43.8% for the geothermal system and by 17.6 % for the solar thermal system compared to the gas boiler system.

*Keywords: Exergy analysis; solar thermal collector; seasonal thermal energy storage; building cluster; heat pump; geothermal borehole heat exchanger; CARNOT, dynamic model; LowEx; low exergy.*

## 1. Introduction

It is useful to apply exergy analysis to community heating systems because "exergy analysis can help locate system nonidealities that either are not identified or misevaluated by energy analysis, as for example the combustion irreversibility" [1]. This combustion irreversibility is demonstrated well by the energy and exergy efficiency of a gas boiler. The energy efficiency can be higher than 90 %, but the exergy efficiency is around 10 %, showing that the potential of gas is not fully used by simply burning it.

At present, more than 30% of the world's energy demand is used in the building sector, of which a large part is needed for heating rooms to approximately 20°C [2]. Room heating is considered as a low quality energy demand, also called low exergy demand [2].

In the course of the Annex 49 of the International Energy Agency, Torío and Schmidt [2] published an exergy assessment guidebook for the built environment and defined low exergy (LowEx) systems as "systems that provide acceptable thermal comfort with minimum exergy destruction". The LowEx approach aims at minimizing the gap between exergy supply and demand. Within their work, the method is applied to several case studies [2]. One outcome is that quasi steady-state analyses are reasonably accurate for investigating different community systems. However, to optimize or study the performance of a system, dynamic analyses are required [2].

Felsmann et al. [3] analyze the influence of low network temperatures on different types of co-generation power plants. They show that lowering the return temperature can improve the systems performance, but there is a trade-off between lowering system temperatures and increasing pump power. Lowering the system temperatures and transforming the system into a LowEx-Net is not always possible due to existing plant components, but is a promising approach for new systems [3].

Bargel [4] presents an exergy analysis model to compare different heat supply system technologies. He concludes that combustion-based technologies have the lowest exergetic efficiency and that auxiliary energy flows cannot be neglected. The author also finds that the relative heat losses of the district heating system increase with increasing insulation standards of the buildings. Because of increasing insulation standards of the building the heat demand decreases. But the heat losses of pipes and other district heating components do not decrease with increasing insulation standards of the buildings. Therefore, the relative heat losses increase. He further concludes that heat networks should operate at low temperatures. Not only because of lower heat losses, but also because high system temperatures eliminate many heat generation technologies with good exergetic efficiency, hence leaving the ones with bad efficiency. In addition, Bargel studies the influence on the system performance of an increasing share of renewable sources in the electrical power generation and indicates that the exergetic efficiency for all system layouts increases [4].

Torío and Schmidt [5] investigate different system concepts in order to improve the performance of a waste heat district heating system. Decreasing the supply

temperatures from 95°C to 57.7 °C increases the exergy efficiency of the system from 32% to 39.3%. Decreasing the return temperature has a similar effect. The energy efficiency remains nearly constant at around 80 % independent of the system configuration [5].

Ozgener et al. [6,7,8] conducted energy and exergy analyses of geothermal district heating systems in the regions of Manisa, Balikesir and Izmir in Turkey. Results of the Balcova district heating system show that exergy losses mainly result from losses in pumps, heat exchangers and re-injection sections of the geothermal water [9].

Çomaklı et al. [10] analyze the oil fired district heating system of the university campus of the Atatürk University, Turkey. They study the exergy losses of the system and find that the total exergy losses relative to the fuel exergy is 16 %. The energy conversion from the power plant to the primary cycle is not within the system boundary.

Bauer et al. [11] give an overview of several solar thermal district heating systems built in Germany and their frame conditions. They conclude that collector fields should have a slope of 35° to 45° to increase solar gains in winter and therefore decrease the required thermal energy storage (TES) capacity. Schmidt et al. [12] also describe several solar thermal district heating systems and emphasize the importance of a low return flow temperature to use the full capacity of the seasonal TES.

In this paper, a dynamic simulation model is developed using the MATLAB/Simulink based toolbox CARNOT [13] and real demand data for 11 buildings with the corresponding weather data for the year 2013 [25]. A district heating system is modeled using as heat supply technology of either a gas boiler, a solar thermal collector system with a seasonal TES or a gas boiler as backup, or geothermal borehole heat exchangers with a heat pump.

The sections below describe the modeled system, the system boundaries, the reference environment, definitions and characteristic numbers, followed by the results and the discussion and conclusion of the paper.

## 2. Methodology
### 2.1 Modeling Software

The system is modeled using the MATLAB/Simulink based toolbox CARNOT. CARNOT stands for **C**onventional **A**nd **R**enewable e**N**ergy systems **O**ptimization **T**oolbox [13]. It was designed for the simulation and analysis of heating systems. In addition to CARNOT, own developments in form of block diagrams and embedded MATLAB functions are also used for the model. The simulations are carried out with variable time steps, simulating a whole year.

### 2.2 System Layout

For a building cluster of 11 buildings, three different heat supply systems are analyzed. The building cluster consists of eight single family houses, one multi-family house, a library and a youth center. Measured demand data for room heating and domestic hot water is available for all 11 buildings in 15 to 30 minute time steps for a whole year. In Figure 1 typical demand curves of three buildings are shown for February 14th 2013. Buildings 3 and 4 are single family houses and building 10 is a library. Building 3 has a low, fluctuating demand. Building 4 is in the middle of the demand range, whereas building 10 has a high demand with a rather smooth curve. The annual heat demand for every building is given in Table 1. All buildings are supplied in parallel with a district heating system from a central heating plant. The supply and return temperatures are $T_s = 50$°C and $T_r = 35$°C, respectively. The district heating system pump is mass flow controlled to meet the desired system temperatures and has a nominal power of 1.1kW. The heat energy demand of the building cluster is 263.7 MWh/a and the corresponding exergy demand is about 30.5 MWh/a. The exergy is calculated using the current outside air as reference state. The three different heat supply systems are a gas boiler system (Figure 2), a solar thermal collector systems with a backup gas boiler (Figure 3) and a geothermal system combined with a heat pump (Figure 4). The district heating system pump and the district heating system itself are not shown in the schematic plans Figure 2, Figure 3, Figure 4.

Table 1. Annual heat demand of the individual buildings.

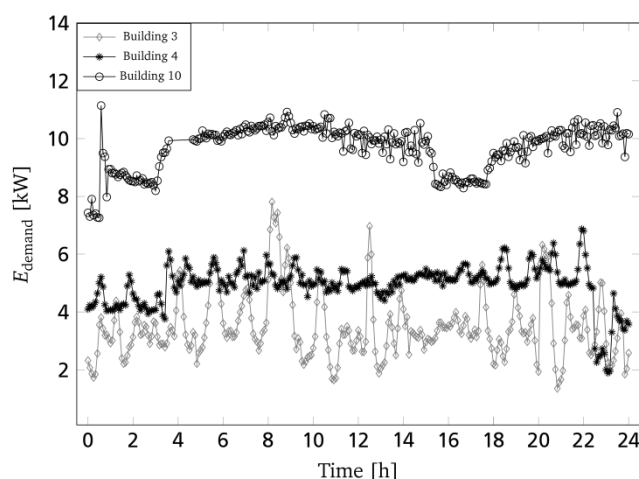| Building | 1 | 2 | 3 | 4 | 5 | 6 |
|---|---|---|---|---|---|---|
| Demand [MWh] | 26.9 | 16.5 | 16.6 | 18.9 | 23.8 | 24.6 |
| Building | 7 | 8 | 9 | 10 | 11 | |
| Demand [MWh] | 16.5 | 14.1 | 36.6 | 35.2 | 34.0 | |



Figure 1. Demand curve for buildings 3, 4 and 10 for February 14th 2013.

#### 2.2.1 Gas Boiler System

The reference case is a gas boiler which provides the building cluster with the required heat via a district heating system Figure 2. The gas boiler nominal power is 140 kW [14] with an efficiency of 86 % and a volume of 10 m³.
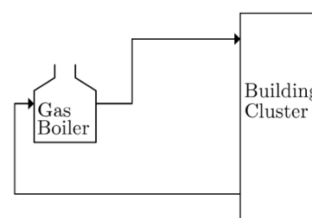


Figure 2. Gas Boiler System.

#### 2.2.2 Solar Thermal Collector System

The solar thermal system (Figure 3) consists of a solar thermal collector with a surface area of 500 m², which is the equivalent area of the overall roof area of the buildings, if all the roofs were facing south at an angle of 40° [14]. A seasonal TES is used to store the heat from the summer months until the heat is needed during the heating period. The TES is modeled as a buried hot water storage tank with a volume of 600 m³. For the solar thermal collector fluid, a

pump with the nominal power of 1.1 kW is used. The pump is also not shown in the schematic plan (Figure 3).
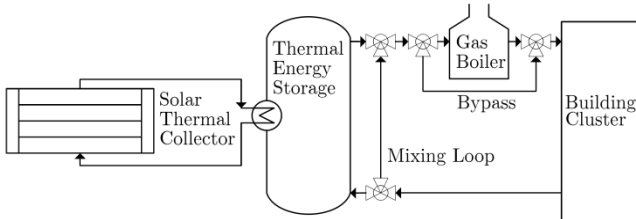


*Figure 3. Solar Thermal System with Seasonal TES and Gas Boiler as backup.*

### 2.2.3 Geothermal System

The geothermal system (Figure 4) has a borehole field with 12 vertical ground-source heat exchangers modeled as double-U-pipe heat exchangers with a depth of 96 m each. The spacing between the boreholes is 9.6 m. The heat pump has a nominal thermal output power of 93 kW [16]. A TES with a volume of 90 m$^3$ is used to decouple the district heating loop from the heat pump in order to enable the use of a heat pump with a smaller nominal power. Since real demand data is used with strong power fluctuations, the TES helps buffer the peaks.
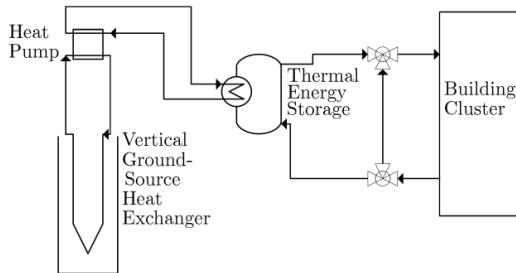


*Figure 4. Geothermal System with Heat Pump.*

### 2.3 Thermal Energy Storage

The TES is included in CARNOT as a finite volume model of a water storage [13]. The TES is a stratified storage tank divided into 15 calculation nodes. For every node an energy balance is calculated. Only heat conduction is taken into account. An effective axial conductivity is used to simulate the convection processes. A heat loss coefficient $k = 0.6$ W/(m$^2$K) between the fluid in the TES and the environment is used for all simulated TES. The heat loss coefficient is chosen iteratively to reach a similar heat loss as in real solar thermal district heating systems, studied in [15]. However, in the parameter study of the solar thermal system, a $k = 0.2$ W/(m$^2$K) is also used as an alternative value [17]. This value is chosen to compare the current TES insulation standard with a theoretically possible heat loss coefficient in an ideal environment. This alternative value is calculated using the equations for a flat plate and a cylindrical shell of the VDI Heat Atlas [18]. The used insulation materials and thickness are taken from [19].

### 2.4 System Boundary

The system boundary is chosen according to the storability criterion [20], which distinguishes between storable and non-storable forms of energy. Hot water is a storable form of energy, whereas electricity is a non-storable form and has to be traced back to the primary energy conversion, where the energy was in a storable form such as coal or gas. The energy flows entering and leaving the system are the following:

- Fuels like natural gas are storable and taken as input into the system.
- Electricity is traced back to the primary energy and exergy input using the German electricity supply mix from 2012. Because of almost identical energy and exergy efficiency for the various types of power plants an energy efficiency $\eta_{el}$ and exergy efficiency $\psi_{el}$ for the electricity production of $\eta_{el} \approx \psi_{el} \approx 0.53$ is used to calculate the actual energy and exergy input into the system [22]. The derivation of $\eta_{el} \approx \psi_{el} \approx 0.53$ is given at the end of this section.
- Solar radiation is non-storable and therefore, the heat gain of the solar thermal collector fluid is taken as input into the system.
- Geothermal heat is storable and is therefore taken as input into the system.
- On the demand side, the system boundary is set to the heat transfer stations at the buildings. The buildings themselves are not within the system boundary.

The derivation of $\eta_{el} \approx \psi_{el} \approx 0.53$ is taken from [22]. $\eta_{el}$ and $\psi_{el}$ can be calculated using:

$$\eta_{el} = \frac{\Sigma_i \sigma_i \eta_i}{\Sigma_i \sigma_i} = \psi_{el} = \frac{\Sigma_i \sigma_i \psi_i}{\Sigma_i \sigma_i}, \qquad (1)$$

where $\sigma_i$ are the percentages of the different kinds of electricity sources on the total electricity supply mix of Germany of the year 2012 [23]. $\eta_i$ and $\psi_i$ are the energy and exergy efficiency of the different kinds of electricity sources. The values for $\sigma_i$, $\eta_i$ and $\psi_i$ are given in Table 2.

*Table 2. Share on the electricity generation and efficiency values of different energy sources*

|  | renewable | oil | lignite | coal | nuclear | gas |
|---|---|---|---|---|---|---|
| $\sigma_i$ | 23 % | 1 % | 26 % | 18 % | 16 % | 12 % |
| $\eta_i$ / $\psi_i$ | 100 % | 52.6 % | 36 % | 36 % [21] | 30 % [21] | 52.6 % [24] |

It is assumed that renewable sources have an efficiency of 100 %, based on the storability criterion. Another assumption is that the transformation efficiency of oil is equal to that of natural gas, and that the transformation efficiency of lignite is equal to that of coal. Other energy sources than the one introduced above are neglected, which is why the sum of the electricity generation shares in Table 2 is 96 % instead of 100 %.

### 2.5 Exergy Definitions

For the exergy definitions the current surrounding air is chosen as the reference environment following the Annex 49 guidebook [2]. The surrounding air data for the year 2013 of the weather station "Mannheim Nord" in Germany is used for the calculations [25].

Four energy/exergy flows enter and one leaves the considered system. For each, the exergy calculation is defined below:

- Exergy of natural gas: To calculate the chemical exergy of natural gas, the quality factor β is used, which is defined for the lower heating value as the quotient of the exergy $EX_{NG}$ and the lower heating value (LHV) of natural gas (NG), $\beta_{NG} = EX_{NG}/LHV$ [26]. In this work, $\beta_{NG,LHV} \approx 1.04$ is used [4].

- Exergy of electricity: The exergy content of electricity is equal to its energy content. However, since electricity is traced back to the primary exergy input the transformation losses also have to be taken into account. Therefore an exergy efficiency of $\psi_{el} = 0.53$ is used to calculate the actual exergy input into the system [22].

- Exergy of solar radiation: The exergy input from solar radiation is calculated using the difference of the exergy content of the solar thermal collector fluid between entering and leaving the solar thermal collector. The equation used to calculate the exergy content of a mass flow is:

$$\dot{EX}_{solar} = -\dot{M}[(h_1 - h_0) - T_0(s_1 - s_0)] , \qquad (2)$$

where $\dot{EX}_{solar}$ is the solar exergy flow, $\dot{M}$ is the fluid mass flow, $h_1$ is the enthalpy at the current state and $h_0$ is the enthalpy at reference state, $T_0$ is the reference temperature, $s_1$ is the entropy at the current state and $s_0$ is the entropy at reference state.

- Exergy of geothermal heat: For the heat entering the system at the borehole the exergy content is calculated using the exergy equation for heat:

$$\dot{EX}_{geothermal} = -\dot{Q}(1 - T_0/T_\infty) , \qquad (3)$$

where $\dot{EX}_{geothermal}$ is the geothermal exergy flow, $\dot{Q}$ is the heat flow from the geothermal heat source, $T_0$ is the reference temperature and $T_\infty$ is the undisturbed ground temperature in half of the depth of the borehole.

- Exergy demand of buildings: The exergy demand is calculated using the difference of the exergy content of the district heating fluid between entering and leaving the transfer stations at the buildings. The equation used to calculate the exergy content of a mass flow is:

$$\dot{EX}_{demand} = -\dot{M}[(h_1 - h_0) - T_0(s_1 - s_0)] , \qquad (4)$$

where $\dot{EX}_{demand}$ is the demand exergy flow, $\dot{M}$ is the fluid mass flow, $h_1$ is the enthalpy at the current state and $h_0$ is the enthalpy at reference state, $T_0$ is the reference temperature, $s_1$ is the entropy at the current state and $s_0$ is the entropy at reference state.

## 2.6 Characteristic Numbers

Several characteristic numbers are used to assess the different systems and results. They are listed in the following paragraphs:

*Energy efficiency*: The system energy efficiency $\eta_{system}$ is defined as the quotient of the energy demand $E_{demand}$ and energy input $E_{input}$:

$$\eta_{system} = E_{demand}/E_{input} \qquad (5)$$

The input into the system varies depending on the system layout. For the gas boiler system, the input is the gas input into the boiler and the primary energy needed to run the pump. For the solar system, the input is the gain through the solar thermal collectors, the gas input into the backup boiler and the primary energy needed to run the pumps. For the geothermal system, the input is the primary energy needed to run the heat pump and the system pumps and the energy gain through the borehole heat exchanger. With these definitions, the overall energy efficiency definition becomes more specific:

$$\eta_{system} = \frac{E_{demand}}{(E_{fossil} + E_{renewable} + E_{\text{TES begin}} - E_{\text{TES end}})} , \qquad (6)$$

where $E_{fossil}$ is the gas input or the fossil energy going into to heat pump and the fluid pumps as introduced in section 2.4, depending on which of the three system layouts is investigated. $E_{renewable}$ is either $E_{solar}$ or $E_{geothermal}$, also dependent on the investigated system layout. $E_{\text{TES begin}}$ is the energy content of the TES at the beginning of the simulation and $E_{\text{TES end}}$ is the energy content of the TES at the end of the simulation.

*Exergy efficiency*: The system exergy efficiency $\psi_{system}$ is defined as the quotient of the exergy demand $EX_{demand}$ and exergy input $EX_{input}$:

$$\psi_{system} = EX_{demand}/EX_{input} , \qquad (7)$$

More specific:

$$\psi_{system} = \frac{EX_{demand}}{(EX_{fossil} + EX_{renewable} + EX_{\text{TES begin}} - EX_{\text{TES end}})} , \qquad (8)$$

where $EX_{fossil}$ is the gas input or the fossil exergy going into to heat pump and the fluid pumps as introduced in section 2.4, depending on which of the three system layouts is investigated. $EX_{renewable}$ is either $EX_{solar}$ or $EX_{geothermal}$, also dependent on the investigated system layout. $EX_{\text{TES begin}}$ is the exergy content of the TES at the beginning of the simulation and $EX_{\text{TES end}}$ is the exergy content of the TES at the end of the simulation.

*Solar coverage*: For the solar thermal system, a solar coverage $\kappa_{solar}$ is calculated which is defined as the quotient of the actual solar heat $E_{\text{TES to district}}$ going into the district heating system after the TES and the demand:

$$\kappa_{solar} = \frac{E_{\text{TES to district}}}{E_{demand}} . \qquad (10)$$

*Exergy efficiency* TES: The exergy efficiency of the seasonal TES $\psi_{\text{TES}}$ in the solar thermal system is defined as:

$$\psi_{\text{TES}} = \frac{EX_{\text{TES to district}}}{(EX_{st\text{ to TES}} + EX_{\text{TES begin}} - EX_{\text{TES end}})} , \qquad (10)$$

where $E_{\text{TES to district}}$ is the exergy of the solar heat going into the district heating system after the TES, $E_{st\text{ to TES}}$ is the exergy of the solar heat going from the solar thermal collectors into the TES, $EX_{\text{TES begin}}$ is the exergy content of the TES at the beginning of the simulation and $EX_{\text{TES end}}$ is the exergy content at the end of the simulation.

## 3. Results

The results presented in this section, are comparisons between the three different system layouts regarding overall exergy input, share of renewable and fossil fuel input and energy and exergy efficiency. For the comparison of the three different systems, the system settings are defined in

section 2.2. Regarding the solar thermal system, the results of a parameter study are given. The investigated parameters are supply and return temperature, TES size and TES heat loss coefficient.

## 3.1 System Comparison

Comparing the energy efficiency of the three different supply scenarios, the gas boiler system has the highest energy efficiency with $\eta_{system,gas} \approx 84\%$ followed by the solar system with $\eta_{system,solar} \approx 70\%$ (Figure 5). The lowest energy efficiency has the geothermal system with $\eta_{system,geo} \approx 65\%$. However, looking at the exergy efficiency, the low exergy efficiency of the gas boiler leaves the two other systems with better results. The geothermal system has the highest exergy efficiency with $\psi_{system,geo} \approx 17\%$, followed by the solar system with $\psi_{system,solar} \approx 12\%$ while the gas boiler system has the lowest exergy efficiency with $\psi_{system,gas} \approx 9\%$ (Figure 5).
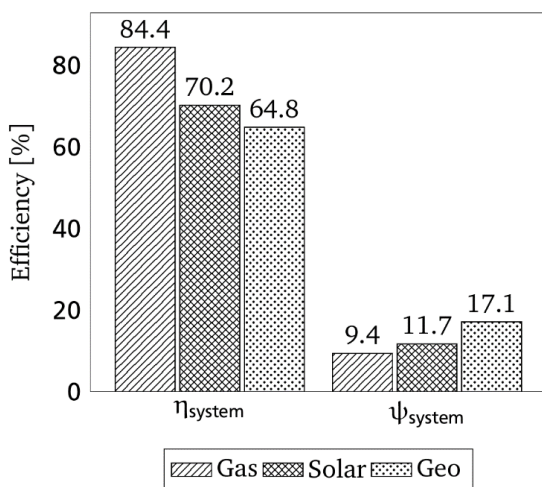


*Figure 5. Energy and Exergy efficiency of the three systems.*
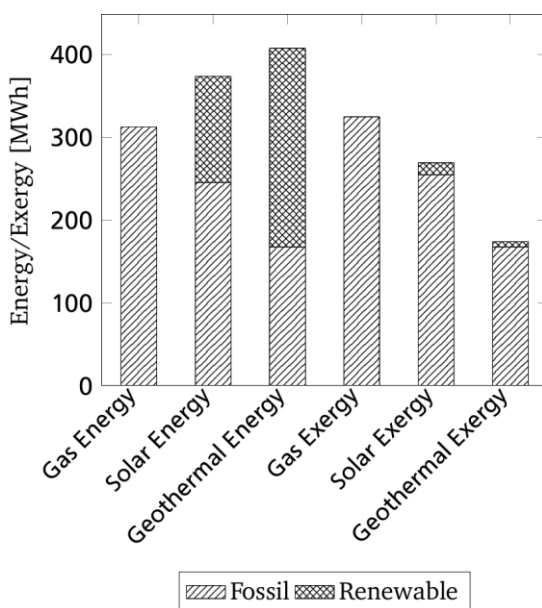


*Figure 6. Energy and Exergy input of the three systems.*

The gas boiler system has the lowest energy input of all three systems (Figure 6). This is due to the high energy efficiency of the boiler. The highest energy input has the geothermal system, followed by the solar system. But, looking at the primary energy input, the gas boiler system uses the most primary energy, since it is the only heat source in this system. The geothermal and the solar system have a higher share of renewable energies, which makes them more sustainable, although they use more energy overall. Looking at the exergy input, the gas boiler system's exergy input of 324.9 MWh/a is about the same as its energy input. The solar system exergy input of 269.2 MWh/a is lower than its energy input, because the exergy content of the hot water leaving the solar thermal collectors is lower than its energy content. The exergy input into the geothermal system of 174.0 MWh/a is lower than half of its energy input, because the heat input from the borehole is very close to the reference temperature, and therefore the exergy content is also very low. Compared to the gas boiler system the use of fossil fuel is 43.8 % lower for the geothermal system and 17.6 % lower for the solar thermal system.

## 3.2 Parameter Study of the Solar System

To study the influence of changing parameters on the performance of the solar system, three parameters have been varied for the solar system. The TES size has been varied from 5 m$^3$ to 1600 m$^3$, the heat loss coefficient of the TES has been set to $k = 0.6$ W/(m$^2$K) and $k = 0.2$ W/(m$^2$K), the latter one being the alternative value introduced in section 2.3. The supply temperatures $T_s$ are 50 °C, 60 °C and 70 °C, with corresponding return temperatures $T_r$ of 35 °, 40 °C and 50 °C. The mass flow for the lowest supply and return temperature is higher than for the other two temperatures. This is necessary to supply the needed heat, because the temperature spread for the lowest temperature is only 15°C instead of 20°C.

The gas exergy input decreases for decreasing supply and return temperatures, independent of TES size and heat loss coefficient $k$ (Figure 7). Two mechanisms mainly lead to lower gas demand for decreasing supply temperatures. One is lower heat losses in the pipes due to lower temperature differences between the fluid and the environment, the other one is a more extensive use of the TES for lower supply temperatures. The TES temperature decreases the longer it is used during the heating period. For lower supply temperatures the TES can be used longer, whereas for higher supply temperatures the TES is sooner too cold to use, therefore effectively decreasing the TES.

For $k = 0.2$ W/(m$^2$K), the gas exergy input decreases with increasing TES size and the gradient is higher for lower temperatures. For a supply temperature of $T_s = 70$°C the exergy input reaches a slight minimum of $EX_{gas\ input} = 262.7$ MWh at a TES size of 1200 m$^3$. For the other two supply temperatures no minimum is reached within the tested TES range.

For $k = 0.6$ W/(m$^2$K), the gas exergy input trend is quite different than for the lower $k$-value. For a supply temperature of $T_s = 50$°C, the exergy input stays rather constant of the range of the TES size, only reaching a slight minimum of $EX_{gas\ input} = 245.6$ MWh at 600 m$^3$. For supply temperatures $T_s$ of 60°C and 70 °C the exergy input reaches a minimum of $EX_{gas\ input} = 258.8$ MWh at 100 m$^3$ and $EX_{gas\ input} = 279.9$ MWh at 50 m$^3$ respectively. After the minimum the exergy input increases again with increasing gradient for increasing supply temperatures. For both k-values and all temperatures the exergy input decreases with a high gradient for the smallest TES sizes.
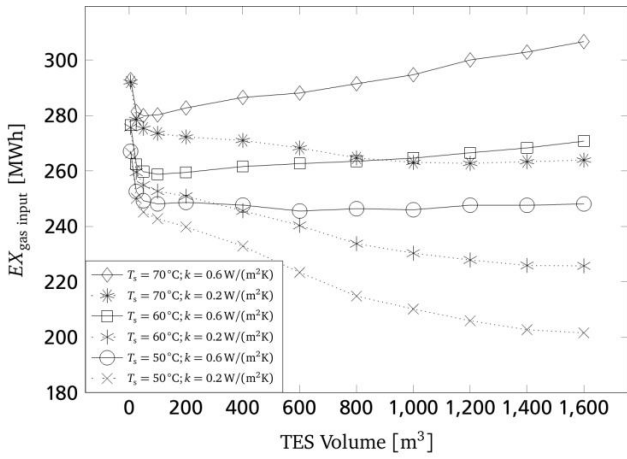
*Figure 7: Exergy input vs. TES size, for the solar thermal system*

The trends for the solar fraction $\kappa_{solar}$ (Figure 8) are in correspondence with the exergy input (Figure 7) because the higher the solar fraction is, the lower the exergy gas input needs to be to cover the demand.
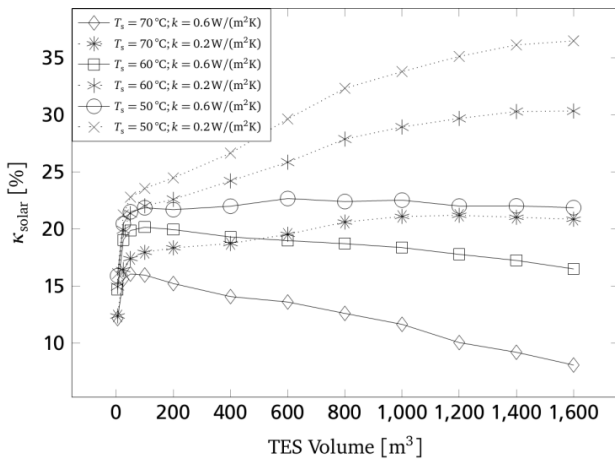


*Figure 8: $\kappa_{solar}$ vs. TES size, for the solar thermal system*

For $k = 0.2$ W/(m²K), $\kappa_{solar}$ increases with increasing TES size and decreasing supply temperature. Only for a supply temperature of $T_s = 70$ °C a maximum of $\kappa_{solar} = 21$ % is reached at a TES size of 1200 m³. For the other two supply temperatures no maximum is reached within the tested TES range. For $k = 0.6$ W/(m²K) and a supply temperature of $T_s = 50$ °C, a slight maximum of $\kappa_{solar} = 22.7$ % is reached at a TES size of 600 m³.

Overall, the exergy efficiency of the TES $\psi_{TES}$ is higher for lower supply temperatures (Figure 9).

For $k = 0.2$ W/(m²K), exergy efficiency trends behave quite similar for all supply temperatures. The exergy efficiency starts above $\psi_{TES} = 90\%$, then decreases with increasing TES size, reaching a minimum around a TES size of 600 m³ to 800 m³ before increasing again with a small gradient.

For $k = 0.6$ W/(m²K), the trends look different. The trends for all three supply temperatures start around $\psi_{TES} = 80$ % and decrease rapidly with increasing TES size, while the gradient increases with increasing supply temperatures. This behavior shows the strong influence of the heat losses on the TES performance.
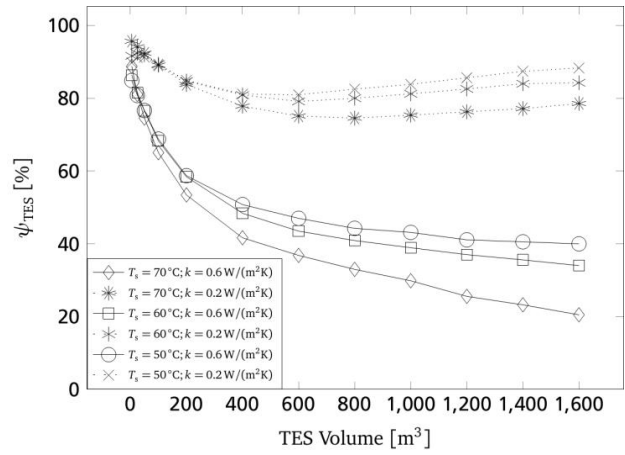


*Figure 9: $\psi_{TES}$ vs. TES size, for the solar thermal system*

## 4. Discussion and Conclusion

Although, the geothermal and the solar system have a higher overall energy input than the gas boiler system, they have a lower fossil energy input. They also have a lower exergy input than the gas boiler system, making them both more suitable to cover the low exergy heating demand of the building cluster. The parameter study of the solar system showed the strong influence of the supply temperature and the heat loss coefficient of the TES on the overall performance of the system. For $k = 0.6$ W/(m²K) best performances are achieved for small TES sizes whereas for $k = 0.2$ W/(m²K), the performance increases with increasing TES sizes, showing that it is crucial to decrease the heat loss coefficient of seasonal TES's to make use of the solar thermal energy. Overall, less gas exergy input is needed with decreasing supply temperatures and decreasing $k$-value.

The open source toolbox CARNOT and the MATLAB/Simulink structure allow for the freedom to model the desired degree of detail, while at the same time keeping the model well structured.

The developed model is capable of dynamically simulating the heat supply of a building cluster. The model can be extended to model different types of buildings and demand profiles, but so far only real demand and weather data is used in the simulations. The supply and return temperatures in the current model are fixed, which does not cover the reality. For all components we have tried to use data from real components out of data sheets, to make the model more realistic. One main advantage of the model is the possibility to study the TES influence in further detail, since the TES is an important component in regard to implementing renewable, fluctuating energy sources. The TES has only been modeled using 15 nodes, due to increasing calculation time with increasing node number. The influence of the number of the TES nodes has also been investigated [17]. The TES efficiency increases slightly with increasing number of nodes, but the overall efficiency is hardly influenced by the number of nodes. Therefore, the number of nodes has been kept small to decrease calculation time.

Future simulations will further investigate the influence of the heat loss coefficient on the TES efficiency in particular and the overall performance in general. Especially the values between $k = 0.2$ W/(m²K) and $k = 0.6$ W/(m²K) will be investigated. Other heat generation technologies such as combined heat and power, and mixed heat supply systems will be implemented into the model as well, to extend the capabilities of the model.

**Nomenclature**

Abbreviations

| | |
|---|---|
| CARNOT | -**C**onventional **A**nd **R**enewable e**N**ergy systems **O**ptimization **T**oolbox |
| LowEx | low exergy |
| TES | thermal energy storage |
| LHV | lower heating value |
| NG | natural gas |

Symbols

| | |
|---|---|
| $E$ | energy (J) |
| $EX$ | exergy (J) |
| $\dot{EX}$ | exergy flow (W) |
| $h$ | specific enthalpie (J/kg) |
| $k$ | heat loss coefficient (W/(m$^2$K)) |
| $\dot{M}$ | mass flow (kg/s) |
| $\dot{Q}$ | heat flow (W) |
| $s$ | specific entropie (J/(kgK)) |
| $T$ | temperature (°C) |

Greek Symbols

| | |
|---|---|
| $\beta$ | quality factor |
| $\eta$ | energy efficiency |
| $\kappa_{solar}$ | solar coverage |
| $\sigma$ | share on electricity generation |
| $\psi$ | exergy efficiency |

Subscript

| | |
|---|---|
| 1 | current state |
| 0 | reference state |
| $\infty$ | distant field |
| i | variable |
| el | electrical |
| r | return |
| s | supply |

**References:**

[1] M. J. Moran, E. Sciubba (1994), "Exergy analysis: Principles and practice," *J. Eng. Gas Turbines Power*, *116*, 285-290.

[2] H. Torío, D. Schmidt (2011), *Detailed Exergy Assessment Guidebook for the Built Environment: ECBCS Annex 49 - Low Exergy Systems for High-Performance Buildings and Communities*, Fraunhofer Verlag, Stuttgart, 2011. http://www.annex49.info/download/Annex49_guideboo g.pdf (accessed 04.03.2013)

[3] C. Felsmann, *LowEx-Fernwärme: Multilevel District Heating ; Zusammenfassung*, TUDpress, Dresden, 2011.

[4] S. Bargel, (2010) *Entwicklung eines exergiebasierten Analysemodells zum umfassenden Technologievergleich von Wärmeversorgungssystemen unter Berücksichtigung des Einflusses einer veränderlichen Außentemperatur*, (PhD Thesis), Ruhr Universität Bochum, Germany: URL http://www-brs.ub.ruhr-uni-bochum.de/netahtml/HSS/Diss/BargelStefan/diss.pdf (accessed 01.03.2013)

[5] H. Torío, D. Schmidt, (2010) "Development of system concepts for improving the performance of a waste heat district heating network with exergy analysis," *Energy and Buildings*, doi:10.1016/j.enbuild.2010.04.002.

[6] L. Ozgener, A. Hepbasli, I. Dincer, "Energy and exergy analysis of geothermal district heating systems: an application," (2005) *Building and Environment,* doi:10.1016/j.buildenv.2004.11.001.

[7] L. Ozgener, A. Hepbasli, I. Dincer, "Energy and exergy analysis of Salihli geothermal district heating system in Manisa, Turkey," (2005) *International Journal of Energy Research,* doi:10.1002/er.1056.

[8] L. Ozgener, A. Hepbasli, I. Dincer, "Energy and exergy analysis of the Gönen geothermal district heating system,Turkey," (2005) *Geothermics,* doi:10.1016/j.geothermics.2005. 06.001.

[9] L. Ozgener, A. Hepbasli, I. Dincer, "Effect of reference state on the performance of energy and exergy evaluation of geothermal district heating systems: Balcova example," (2006) *Building and Environment,* doi:10.1016/j.buildenv.2005.03.007.

[10] K. Çomaklı, B. Yüksel, Ö. Çomaklı, "Evaluation of energy and exergy losses in district heating network," (2004) *Applied Thermal Engineering,* doi:10.1016/j. applthermaleng.2003.11.014.

[11] D. Bauer, W. Heidemann, H. Müller-Steinhagen, *Central solar heating plants with seasonal heat storage* (2007). Available: URL http://www.itw.uni-stuttgart.de/dokumente/Publikationen/publikationen_07-07.pdf (accessed 13.10.2015)

[12] T. Schmidt, D. Mangold, H. Müller-Steinhagen, (2004) "Central solar heating plants with seasonal storage in Germany," *Solar Energy,* doi:10.1016/j.solener.2003. 07.025.

[13] Solar Institut Jülich Germany, CARNOT 5.3: Matlab simulink toolbox extension (1999).

[14] Robert Klemmer (2014), *Modellierung und Analyse von Wärmespeicherszenarien in CARNOT*, (MSc Thesis), TU Darmstadt, Germany.

[15] M. Bodmann, D. Mangold, J. Nußbicker, S. Raab, A. Schenke und T. Schmidt, *Solar unterstützte Nahwärme und Langzeit-Wärmespeicher: Forschungsbericht zum BMWA / BMU-Vorhaben, Solar- und Wärmetechnik Stuttgart (SWT)* (2005). Available: URL http://www.solites.de/download/literatur/AB-SUN%20 V%20FKZ%200329607F.pdf (accessed 27.10.2015)

[16] Hendryk Engelbart (2015), *Erweiterung des Gebäudegruppenmodells in CARNOT*, (MSc Thesis), TU Darmstadt, Germany.

[17] Andreas Riedel (2015), *Sensitivitätsanalysen eines Wärmeversorgungsmodells einer Gebäudegruppe*, (Bachelor-Thesis), TU Darmstadt, Germany.

[18] VDI-Gesellschaft Verfahrenstechnik und Chemieingenieurwesen (GVC) (Ed.), *VDI Heat Atlas*,

*2nd Ed.* Springer, Berlin and Heidelberg, 2010. doi:10.1007/978-3-540-77877-6.

[19] T. Schmidt, M. Benner, W. Heidemann, H. Müller-Steinhagen, *Saisonale Wärmespeicher - aktuelle Speichertechnologien und Entwicklungen bei Heißwasser-Wärmespeichern* (2003). Available: URL http://www.swt-stuttgart.de/SWT-Forschung/Veroeffentlichungen/Puplic/03-01.pdf (accessed 26.11.2015)

[20] A. Jentsch, *A novel exergy-based concept of thermodynamic quality and its application to energy system evaluation and process analysis*, (PhD Thesis), TU Berlin, Germany 2010. Available: URL http://opus.kobv.de/tuberlin/volltexte/2010/2576/ (accessed 01.03.2013)

[21] M. A. Rosen, "Energy- and exergy-based comparison of coal-fired and nuclear steam power plants," (2001) *Exergy, An International Journal*, doi:10.1016/S1164-0235(01) 00024-3.

[22] Nico Schmitt, *Exergy analysis and life-cycle-assessment of an energy system on object level in settlement areas*, (Master-Thesis), (2014), TU Darmstadt, Germany.

[23] Agentur für Erneuerbare Energien, *Strommix in Deutschland* (2012). Available: URL http.//www.unendlich-viel-energie.de/mediathek/grafiken?cont=217 (accessed 02.01.2014)

[24] G. P. Hammond, Ondo Akwe, Serge S., "Thermodynamic and related analysis of natural gas combined cycle power plants with and without carbon sequestration," (2007) *Int. J. Energy Research,* doi:10.1002/er.1328.

[25] Landesanstalt für Umwelt Messungen und Naturschutz, *Wetterdaten,* (2013), Available: URL http://udo.lubw.baden-wuerttemberg.de/public/ (accessed 23.10.2015)

[26] A. Hepbasli, "A study on estimating the energetic and exergetic prices of various residential energy sources," (2008) *Energy Buildings,* doi:10.1016/j.enbuild.2007.01.023.